A Thesis

for the Degree of Master of Science

Synbiotics with curcumin-loaded pullulan nanoparticles induce anti-bacterial and intestinal immune activities

커큐민 담지 플루란 나노입자 활용

신바이오틱스의 장내 항균 및 면역증진

August 2021

By

Seo Kyung Kim

School of Agricultural Biotechnology

Graduate School

Seoul National University

이 학 석 사 학 위 논 문

Synbiotics with curcumin-loaded pullulan nanoparticles induce anti-bacterial and intestinal immune activities

커큐민 담지 플루란 나노입자 활용 신바이오틱스의 장내 항균 및 면역증진

지도교수 윤철희
이 논문을 이학석사학위논문으로 제출함

2021 년 04 월

서울대학교 대학원
농생명공학부
김 서 경

김서경의 석사학위논문을 인준함
2021 년 06 월

위 원 장 박 주 홍
부위원장 윤 철 희
위 원 유 경 로

Abstract

Inflammatory bowel disease (IBD) is a group of chronic inflammatory disease of the gastrointestinal tract. There have been many treatments suggested but the way to directly cure IBD has not been fully discovered. Therefore, studies of probiotics, and prebiotics, called as the 'synbiotics' treated in order to maintain the microbial diversity have been carried on actively. In this study, curcumin-loaded phthalyl pullulan nanoparticles (PPNs), developed as prebiotics, were internalized into *Lactobacillus plantarum* (*L. plantarum*). The results showed that internalization induced mild stress to *L. plantarum* leading to a production and secretion of plantaricin. Furthermore, there was an increase of anti-microbial effects to *L. monocytogenes* and *E. coli*.

Anti-inflammatory effects of *L. plantarum* internalized with curcumin-loaded PPNs were shown in the intestine of DSS-induced colitis model. They exerted protective effect against the gut microbiota disruption in mouse with colitis condition. Collectively, *L. plantarum* internalized with curcumin-loaded PPNs improved microbial diversity and showed potential in enhancing the immune activities in the intestine.

keywords: nanoparticles, synbiotics, IBD

Contents

List of Figures

Review of Literature

Materials and Method

Results

List of Tables

Review of Literature

Materials and Method

Results

List of Abbreviations

AMP	Anti-microbial peptide
BHI	Brain heart infusion
BMDC	Bone marrow-derived dendritic cell
CD	Crohn's Disease
CLSM	Confocal laser scanning microscopy
DC	Dendritic cell
DLS	Dynamic light scattering
DMAP	Dimethylaminopyridine
DSS	Dextran sulfate sodium
E. coli	*Escherichia coli*
ELS	Electrophoretic light scattering
F/B	Fermicutes/Bacteriodetes
FE-SEM	Field-emission scanning electron microscope
FITC	Fluorescence isothiocyanate
GI	Gastrointestinal
IBD	Inflammatory bowel disease
IEC	Intestinal epithelial cell
Ig	Immunoglobulin
LAB	Lactic acid bacteria
LB	Lysogeny broth

L. monocytogenes	*Listeria monocytogenes*
L. plantarum	*Lactobacillus plantarum*
LPCP	*L. plantarum* internalized with curcumin-loaded PPNs
MHC	Major histocompatibility complex
MRS	Man, Rogosa and Sharpe
NMR	Nuclear magnetic resonance
PFA	Paraformaldehyde
PPN	Phthalyl pullulan nanoparticles
qRT-PCR	Quantitative real time polymerase chain reaction
TEM	Transmission electron microscopy
UC	Ulcerative colitis

I. Review of Literature

The contents herewith will be published elsewhere

as a partial fulfillment of Seo Kyung Kim's M. Sc. program

1. Definition and chemical properties of curcumin

Curcumin (diferuloylmethane) is a deep orange yellow colored powder in which their property is an amphiphile [1], possessing hydrophobic and lipophilic (Figure 1) properties. It is the major ingredient of the rhizome of the plant called *curcuma longa*, commonly known as turmeric, belonging to the *Zingiberaceae* family. Curcumin was first isolated from turmeric in 1815 [2] with only a few characteristics known until in the 1990s when Singh et al. [3] reported an anti-cancer effect of curcumin which grew the interest rapidly. Traditionally, curcumin has been used as spice, condiment, in cosmetics, textile, and medicine [4]. It has been shown over the last few decades that curcumin has potential anti-microbial, anti-fungal, anti-inflammatory and anti-cancer effects [5]. Curcumin can suppress inflammatory responses and contribute to the alleviation of variety of inflammatory diseases including type 2 diabetes [6], asthma [7], cardiovascular diseases, and inflammatory bowel diseases [8]. Curcumin

modulates multiple cellular and molecular targets [9] in accordance with biological activities including inhibition of NFκB, JAK/STAT/SOCS signaling pathways [10]. Therefore, curcumin has been suggested for their therapeutic potential in alleviating inflammatory symptoms.

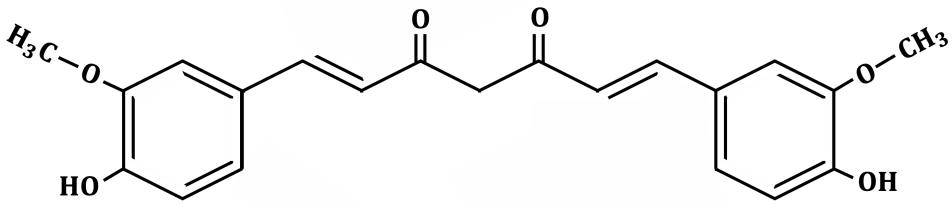

Figure 1. Structural formula of curcumin.

The chemical formula of curcumin is $C_{21}H_{20}O_6$ with many aromatic rings which make them insoluble in water. The phenol rings of curcumin cause a hydrophobic nature [11] with a low solubility, less distribution properties and low absorption rate in the body. Nanoparticles are known to enhance the bioavailability of hydrophobic drugs [12]. For instance, curcumin-loaded nanoparticles have been suggested for their ability to enhance the absorption and distribution in the body in animals [13].

2. Enhancement of bioavailability using polymeric nanoparticles

The limitations of conventional therapeutics can be overcome with beneficial properties of nanoparticles [14]. In case of curcumin, these confinements include poor water solubility, aggregating properties, systemic toxicity, non-specific and non-local biodistribution and the susceptibility to physiological degradation [15]. These can be supplemented by the application of the properties of nanoparticles as following; Nanoparticles can be easily designed and prepared and enables increase of stability [16] Moreover, they can be tunable in size [17] and shape [18], and efficiency can be increased by the large surface area to volume ratio [19] and to add, their surface can be functionalized for their specific distribution [20]. Most importantly, physiologically active and hydrophilic substances are difficult to deliver into the cells but when loaded on nanoparticles, they gain the access to enter the cells relatively easily through endocytosis [21]. In the case of the physiologically active and hydrophobic substances which are not soluble in water are dissolved in an organic solvent, and then transferred into the cells by diffusion. However, it is difficult to control the release of the content and potential trace of toxicity from the organic solvent. Use of nanoparticles has been suggested for loading and controlling the time and spatial release of such substance [22].

Table 1. Beneficial properties of nanoparticles to overcome the limitations of conventional therapeutics.

Limitations of conventional therapeutics	Beneficial properties of nanoparticles
Poor water solubility	High surface to volume ratio
Aggregating properties	Easier entrance into biological membrane
Systemic toxicity	Stable in size, nature, shape, zeta potential
Non-specific biodistribution	High surface to volume ratio
Susceptible to physiological degradation	Easier entrance into biological membrane

3. Inflammatory bowel disease

3-1. Dextran sodium sulfate-induced colitis in mice

Inflammatory bowel disease (IBD) is defined as a group of chronic inflammatory disease of the gastrointestinal (GI) tract. Even though the causes of IBD are specified ambiguously, it's etiopathogenesis can be explained by multiple reasons. It is generally accepted that IBD is a result of immune response, especially in genetically susceptible or immunocompromised individuals, against the microbial and environmental factors including smoking, drug intake, pollution, diet [23] and food additives and among others [24]. Ulcerative colitis (UC) and Crohn's disease (CD) are common subtypes of the IBD and their

symptoms include diarrhea, abdominal pain, fever, fatigue, bloody stool, reduced appetite, and weight loss. Although there is a no direct cure for IBD, various treatments such as anti-diarrheal medication, pain reliever, antibiotics, immunosuppressant are suggested and, in severe cases, biological therapies and surgeries can be performed.

In mouse model, colitis can be induced by dextran sulfate sodium (DSS) which are sulfated polysaccharide that is toxic to especially the epithelium. According to the period of the DSS implementation by oral treatment, they can induce either acute or chronic colitis. Both acute and chronic models of DSS-induced intestinal inflammation could be achieved by regulating either the concentration of DSS or the frequency of administration, or both [25].

3-2. Intestinal barrier function

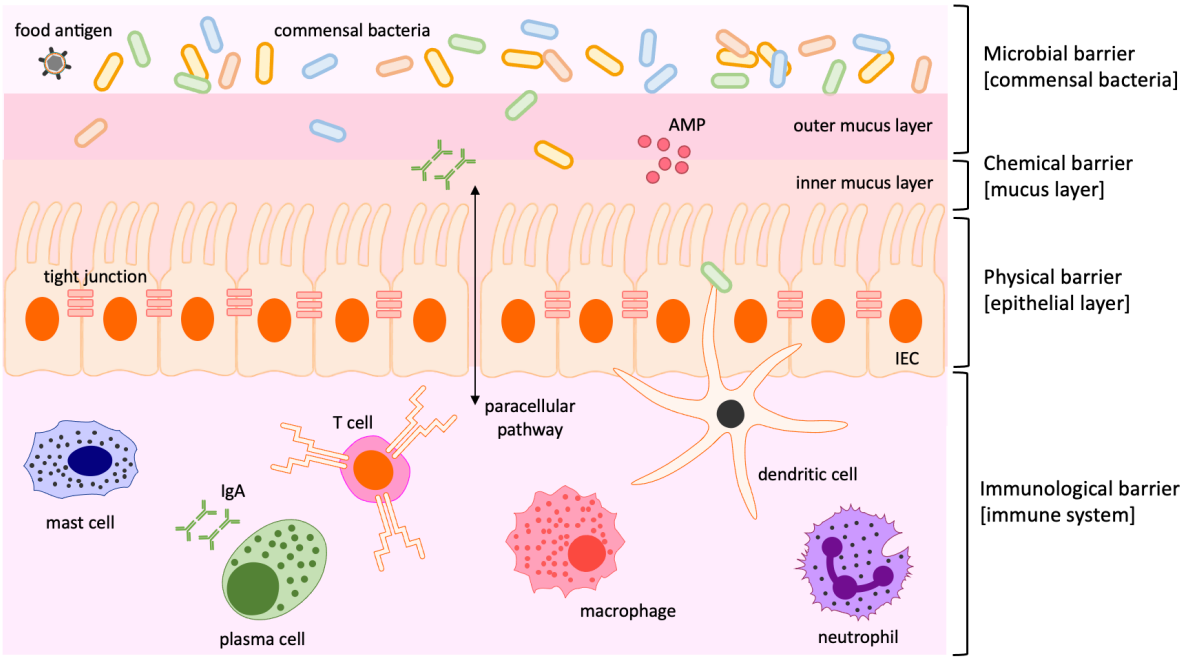

Figure 2. Schematic diagram of the intestinal barrier.

The intestinal lumen is the first line of defense from exogenous antigens and microbial products. The antigens include food particles, toxins, viruses, microorganisms, drugs etc. and when homeostasis in the gut is broken, the antigens could penetrate through unwanted manner at the intestinal barrier system. As shown in Figure 2, intestinal barrier can be classified into four layers, microbial, chemical, physical, and immunological barriers [26]. First, the microbial layer containing the intestinal lumen and the outer mucus layer, is

where food antigen, anti-microbial peptide (AMP), secreted immunoglobulin (Ig) A and commensal bacteria exist. Commensal bacteria prevent the colonization of exogenous antigens and noxious bacteria by competing for nutrition and by secreting AMP in order to suppress and kill them. Second, the chemical barrier is the inner mucus layer where the mucus prevents exogeneous pathogens from adhering to the epithelium and blocks their penetration into the tissues beneath. Third, the intestinal epithelial cell (IEC) layer separates the outer environment from the internal environment forming a physical barrier. IECs are continuous and forming tight junctions to seal them together. When the homeostasis is disturbed, pathogens may enter the body as the paracellular pathway is left ajar. The last, under the IECs, the immunological barrier is formed where various immune cell types such as dendritic cells (DCs), macrophages, mast cells, T cells, and plasma cells exist. Macrophages directly kill the penetrated pathogens, plasma cells produce and secrete IgA, and dendritic cells which capture the antigen, deliver the signal (i.e., major histocompatibility complex (MHC) class I or II) to the T cells bringing up antigen recognition and further immune responses.

4. Synbiotics

4-1. Probiotics

Probiotics are live microorganism that can give health benefit to the host when administered at adequate amount (FAO/WHO, 2001). Probiotics can not only affect pathogens directly by producing anti-microbial substances represented by bacteriocins but also modulate host immune defense responses such as stimulating the innate immune response, increasing the intercellular integrity of the tight junction, producing metabolites such as short chain fatty acids. Among the numerous microorganisms defined as probiotics, many are lactic acid bacteria (LAB) and bacilli. *Lactobacillus plantarum* has been characterized as a probiotic and known for their particular anti-oxidant activities [27]. It has been suggested that they may play an important role in prevention and cure of infectious and inflammatory diseases of the intestine and to induce production of IL-10 in macrophages [28] and dendritic cells [29] usually working along with adaptive immune cells, but their mode of action mechanisms is yet to be further studied.

4-2. Prebiotics

Prebiotics are defined as substances that are non-digestible, but can stimulate the growth and/or activity of other microorganisms in the GI tract in order to exert beneficial effects on the host. The current definition is being expanded to ‘materials that could be selectively conjugated by microorganisms in the host’s GI tract exerting a health benefit [30], yet the definition and range of prebiotics are still controversial. This is due to the potential prebiotic agent that either selectively stimulate or stimulates a limited number of host microorganisms.

Pullulan (Figure 3) is a polymer of maltotriose subunits that are synthesized and secreted from the fungus *Aureobasidium pullulans*.

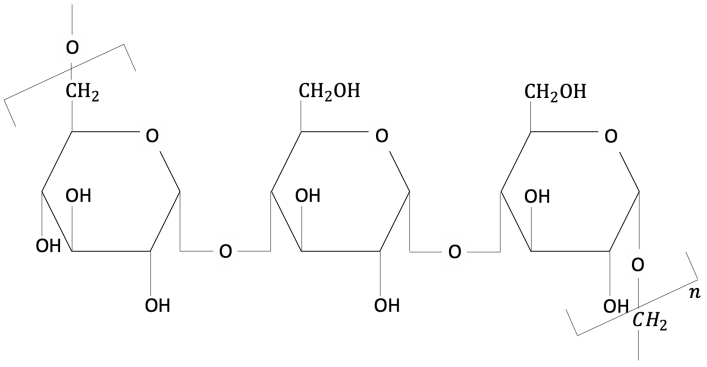

Figure 3. Chemical structure of pullulan.

Pullulan is an α-1,6 linked polymer. α-amylase and glucoamylase hydrolyze the high molecular weight pullulan very slowly and therefore, pullulan is considered as a non-digestible carbohydrate [31] which satisfies the terms of prebiotics. Pullulan, here in this study was used to synthesize polymeric nanoparticles using hydrophobic interactions and the 'self-assembly' process [32] and curcumin, as an immunomodulator, was loaded on to this nanoparticle. When the curcumin-loaded nanoparticles were internalized into the microbiota they induce a mild stress and led to the change on the composition of the intestinal microbiota by secreting antimicrobial substances.

4-3. Bacteriocin

The advantage of using *Lactobacillus plantarum* as probiotics is that they can produce self-defensing antimicrobial substances, for instance bacteriocin and lactic acid. With aid of these substances, *Lactobacillus plantarum* can survive in the gastrointestinal tract's environment affecting the host's immune responses. Bacteriocins, produced by both Gram-positive and Gram-negative bacteria, are proteinaceous substances that has antimicrobial properties, generally inhibiting the growth of similar or closely related species [33]. Bacteriocins can be classified into 4 classes according to their molecular size, mode of specificity, properties of the modified amino acids, morphological characteristics and their working mechanism [34]. *Lactobacillus plantarum* strains generally produce plantaricin EF, plantaricin JK, plantaricin S, and plantaricin A that are included in class 2 bacteriocins which are non-lanthionine containing bacteriocins with less than 10 kDa and heat stable.

II. Introduction

Inflammatory bowel disease (IBD), a steadily increasing disease worldwide [35], includes Crohn's disease and ulcerative colitis. It has been expanding its emerging situation largely due to westernized lifestyle [36] and other environmental factors such as stress, smoking [37] and diet [23]. IBD is a group of chronic inflammatory disease of the intestinal tract [38], where the large number of researches to find the direct cure to IBD have been performed with antibiotic treatment [39] and biological surgeries [40]. However, as a disease that repeats cure and relapse, direct cures to IBD are yet to be found and needs a further investigation.

It has been suggested accumulation and penetration of pathobionts [41] lead to disrupted microbial diversity and often the loss of beneficial symbionts under IBD condition. Probiotics treatment, suppressing pro-inflammatory condition[42], strengthen the intestinal integrity [43], and maintain the diversity of the microbial composition in the intestine, has been reported as a potential cure in animals with IBD [44]. Prebiotics, non-digestible materials that stimulate the activities of probiotics in the gastrointestinal tract to confer favorable health effects on the host [30], are known to enhance the beneficial functions of probiotics in inflammatory circumstances [45, 46]. Pullulan nanoparticles, as

prebiotics, enhance the antimicrobial effects of *L. plantarum* [32]. On the other hand, *L. plantarum* has been suggested to confer protective effects against IBD [47]. L. *plantarum* inhibits proinflammatory cytokines during the development of colitis causing amelioration of colitis-induced pathophysiology [47]. Therefore, the protective effects of *L. plantarum* in the form of synbiotics are sounding. *Lactobacillus rhamnosus* strain GG [48] and *L. paracasei* B21060 [49] each treated with prebiotics that works as synbiotics show ameliorating effects in animals with colitis. Exact mechanisms and function of symbiotic supplementation still need to be further investigated, however, there are many studies suggesting the benefits conferred by the synbiotics.

In this study, mice with colitis were treated with curcumin-loaded nanoparticles that were internalized into *L. plantarum*. The present study highlighted that curcumin-loaded PPNs acting as prebiotics to L. *plantarum* enhanced anti-microbial activities of L. *plantarum* and their contribution to anti-inflammatory effects in mice with colitis, ameliorating the symptoms.

III. Materials and method

1. Animal

Female, 6-week old, C57BL/6 mice were obtained from Orient Bio (Gapyeong, South Korea). The mice were housed in sterilized cages in a controlled environment with a 12 h light-dark cycle. All the experimental procedures were carried out in accordance with the Animal Use and Care protocol approved by the Institutional Animal Care and Use Committee (IACUC) at Seoul National University, Seoul, Korea (Approval No. SNU-200902-3-1)

2. Materials

All the materials and chemicals used in this study were provided from Sigma-Aldrich (St. Louis, Mo, USA) and otherwise, they were stated. Lactobacilli MRS broth and agar, BBL MacConkey agar, brain heart infusion (BHI) broth and Lysogeny broth (LB) agar were purchased from BD Difco (Sparks, MD, USA) for bacterial cultures.

3. Synthesis of phthalyl pullulan nanoparticles

Phthalyl pullulan nanoparticles (PPNs) were synthesized based on the previous study [32], with a slight modification. One gram of pullulan was dissolved in 10

mL of N,N-Dimethylformamide (DMF). 2.64 g of phthalic anhydride was added to the solution at 9:1 ratio of phthalic anhydride to pullulan and 0.1mol-% dimethylaminopyridine (DMAP) per pullulan sugar residue was added as a catalyst. The reaction was performed at 54 ℃ for 48 hours under nitrogen bubbling for 15 minutes. After the reaction, the materials were dialyzed first at 4 ℃ in DMF for 24 hours in order to remove the unreacted phthalic anhydride. And then, they were dialyzed at distilled water at 4 ℃ for 24 hours in order to form self-assembled phthalic pullulan nanoparticles. Unreacted pullulan was removed by ultracentrifugation and the pellet was freeze-dried and stored at -20 ℃ till use.

4. Characterization of PPNs

The substitution rate of phthalic anhydride was confirmed by 600MHz ^{1}H-Nuclear magnetic resonance (NMR) spectroscopy (AVANCE 600, Bruker, Germany). The morphologies of PPNs were checked using transmission electron microscopy (TEM, LIBRA 120, Carl Zeiss, Germany) and the surface morphology was observed using a field-emission scanning electron microscope (FE-SEM, SUPRA 55VP-SEM, Carl Zeiss, Oberkochen, Germany). The particle size of PPNs was measured by dynamic light scattering (DLS) spectrophotometer (DLS-7000, Otsuka Electronics, Japan) and the zeta potential was examined by

using electrophoretic light scattering (ELS) spectrophotometer (ELS-8000, Otsuka Electronics, Japan).

5. Preparation and characterization of curcumin-loaded PPNs

One milligram of PPN was dissolved in 10 mL of DMF and dialyzed in distilled water for 24 hours at 4 ℃ with the dialysis tube (Repligen Cororation, molecular weight cut-off with 12,000 to 14,000 kD) and freeze-dried. Afterwards, the final concentration of 10 μM of curcumin was loaded at 0.05 wt.% of PPNs. The loading content of curcumin in PPNs were calculated using the following equation.

$$\text{Loading content (\%)} = \frac{\text{amount of curcumin in the PPNs}}{\text{amount of curcumin-loaded PPNs}} \times 100\ \%$$

Size of the curcumin-loaded PPNs was measured by DLS (DLS-7000, Otsuka Electronics, Japan) and the difference on the intensity of the curcumin-loaded PPNs was examined by using TEM (TEM, LIBRA 120, Carl Zeiss, Germany).

6. Confirmation of the internalization of PPNs into *Lactobacillus plantarum*

Fluorescence isothiocyanate (FITC)-labeled PPNs were prepared ahead. 100 mg of PPNs were dissolved in 1 mL Dimethyl sulfoxide (DMSO) with 5 mg of FITC

and they were stirred for 3 hours at room temperature. This solution was dialyzed with distilled water for 24 hours at 4 ℃ and the pellet was harvested by ultracentrifugation and the freeze-dried to be stored at -20 ℃ till use.

The internalization of PPNs in *L. plantarum* was observed using confocal laser scanning microscopy (CLSM, SP8X STED, Leica, Wetzlar, Germany) and the fluorescent microscope (Nikon Eclipse E1 microscope, with a Plan Fluor 100x/1.30 NA oil immersion objective). *L. plantarum* was treated with 0.5% (w/v) FITC-labeled PPNs for 1 hour at 37 ℃. The samples were washed with PBS and fixed using 10% paraformaldehyde. The internalization of PPNs into *L. plantarum*177 was fully confirmed with observation by Z-section mode in CLSM.

7. Analysis of genes related to the stress response and levels of plantaricin-related genes in *L. plantarum* treated with curcumin-loaded nanoparticles by quantitative real-time PCR

RNA extraction was performed using the Trizol Max™ Bacterial RNA Isolation Kit purchased from Thermo-Fisher Scientific Inc. (Waltham, MA, USA). Total RNA extraction was conducted according to the manufacturer's instruction. *L. plantarum* was treated with PPNs curcumin, and curcumin-loaded PPNs. After the isolation of RNA, cDNA was synthesized with random primers (500 μg/ml),

dNTP (10 mM), 5X first strand buffer, DTT (0.1 M), oligo dT, M-MLV reverse transcriptase (Invitrogen, USA). Quantities of all targets in tested samples were normalized to the corresponding 16s rRNA levels. And Real-time RT-PCR was performed with the SYBR Green PCR Master Mix using StepOnePlus Real-Time PCR System (both from Applied Biosystems, USA). Relative quantification of target genes was calculated using the $2^{-\Delta\Delta Ct}$ method. Primer sequences used for Real time quantitative PCR are shown in Table 2.

Table 2. RT-PCR primers of *L. plantarum*.

Gene	Forward (5' → 3')	Reverse (5' → 3')
planS	GCCTTACCAGCGTAATGCCC	CTGGTGATGCAATCGTTAGTTT
dnaK	ATTAACGGACATTCCAGCGG	TTGGCCTTTTTGTTCTGCCG
dnaJ	GGAACGAATGGTGGTGGCCCTTA	CTAGACGCACCCACCACAAA
16S rRNA	GATGCGTAGCCGACCTGAGA	TCCATCAGACTTGCGTCCATT

Total RNA was also extracted from perfused intestinal tissues by Trizol reagent (Thermo Fisher Scientific) and isolated by adding chloroform. This step was followed by centrifugation at 4 ℃, 12,000 g for 15 minutes and addition of isopropanol for 10 minutes at room temperature for RNA precipitation. RNA pellet was obtained by washing with 75 % ethanol and air dried for 10-15 minutes then resuspended with DEPC water and quantified with NanoDrop (Amersham Bioscience, USA) at A260/280. cDNA synthesis and Real-time RT-PCR were performed as aforementioned. Primer sequences used for Real time quantitative PCR are shown in Table 3.

Table 3. RT-PCR primers of mice.

Gene	Forward (5' → 3')	Reverse (5' → 3')
IL-10	CAGCCGGGAAGACAATAACTG	CCGCAGCTCTAGGAGCATGT
IL-17A	CAGCAGCGATCATCCCTCAAAG	CAGGACCAGGATCTCTTGCTG
IL-6	GAGGATACCACTCCCAACAGACC	AAGTGCATCATCGTTGTTCATACA
Occludin	ATCAACAAAGGCAACTCT	GCAGCAGCCATGTACTCT
ZO-1	GAGTTTGATAGTGGCGTT	GTGGGAGGATGCTGTTGT

8. Bacterial culture

E. coli K99 and *L. monocytogenes* were used as representative Gram-negative and Gram-positive pathogens, respectively. MRS and BHI were used for *L. plantarum*, *E. coli* K99, and *L. monocytogenes*, respectively. All bacteria cultures were incubated at 37℃ in a shaking incubator (250 rpm) for 24 hours prior to experimental procedures or stored at -70℃ in 15% glycerol for further use.

9. Co-culture assay and agar diffusion test for antimicrobial ability

Antimicrobial activity of *L. plantarum* against *E. coli* and *L. monocytogenes* was determined using co-culture assays [50] and agar diffusion tests [51], with a minor modification. Briefly, to compare the antimicrobial activity of *L. plantarum* against *E. coli* by co-culture assay, 2.0×10^6 CFU/ml of *E. coli* was co-cultured with 2.0×10^5 CFU/ml of *L. plantarum* treated with or without 0.5%

(w/v) PPNs or curcumin-loaded PPNs in MRS broth for 8 hours at 37 ℃ under aerobic conditions in a shaking incubator (250 rpm). The antimicrobial activity was determined by the survival rate of *E. coli*. The co-cultured samples were spread on MacConkey agar and incubated for 24 hours at 37℃, and the number of *E. coli* colonies was counted. The antimicrobial activity of *L. plantarum* against *L. monocytogenes* was also determined by co-culture assay. *L. plantarum* and *L. monocytogenes* were co-cultured in BHI broth under similar conditions as described above. Finally, the co-cultured samples were spread on Oxford agar, and the number of *L. monocytogenes* colonies was counted.

The agar diffusion test was used to determine either *L. plantarum* treated with PPNs, curcumin, or curcumin-loaded PPNs were able to inhibit the growth of pathogens on an agar plate. First, 100 μl *E. coli* was spread on to LB agar. A paper disk was placed on the *E. coli*-spread plate, then 120 μl of *L. plantarum* cultured with either PPNs, curcumin, or curcumin-loaded PPNs for 8 hours was dropped onto the paper disk. After drying at room temperature, the plate was cultured overnight at 37℃. The zone of inhibition, measured by its diameter, against *E. coli* growth was used as an antimicrobial activity. The same protocols were followed to test the inhibitory effect of *L. plantarum* treated with or without

0.5% (w/v) PPNs or curcumin-loaded PPNs on *L. monocytogenes* growth on BHI agar plates.

10. 16s rRNA sequencing

Fecal samples from the experimental groups were delivered to NICEM (National Instrumentation Center for Environmental Management, Seoul, Korea) for V416S gene sequencing using and Illumia MiSeq platform and a microbial profiling report.

11. Chronic dextran sodium sulfate (DSS)-induced colitis model in mice

To induce acute colitis, mice were provided 2.5% (w/v) DSS (molecular mass = 36-50 kDa, MP Biomedicals) in drinking water for 7 days, followed by 7 days of access to regular drinking water. Daily clinical assessment of DSS-treated animals included body weight loss measurement, stool consistency, and detection of blood in the stool. Experimental samples were collected on day 7 of DSS treatment.

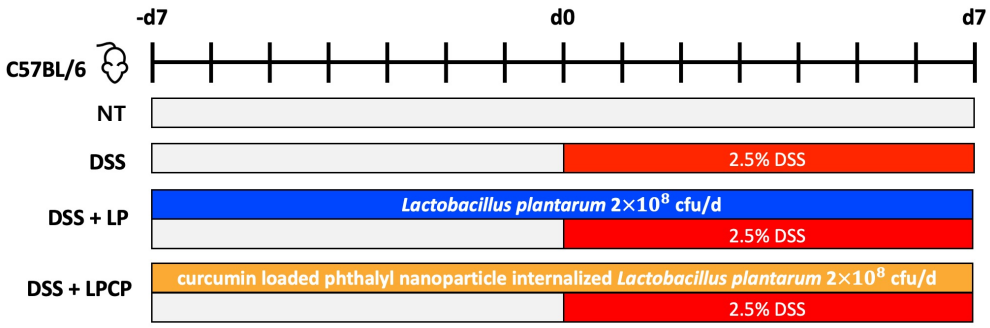

Figure 4. Experimental schedule and group organization.

L. plantarum internalized with curcumin-loaded PPNs (LPCP)

12. Histology

For histological analysis, large intestine tissues taken from mouse were perfused and fixed with 4 % paraformaldehyde and embedded into paraffin block for hematoxylin and eosin (H&E) staining. Samples were examined under the light microscopy (Leica Microsystems, Wetzlar, Germany). All clinical and histological evaluations were performed in blinded manner.

13. Statistical analysis

Data are presented as the mean ± SEM of three independent experiments. The statistical significance was analyzed between each group by one-way analysis of variance (ANOVA) followed by Tukey's test for multiple comparisons.

IV. Results

1. Synthesis and characterization of PPNs

The schematic procedure for the reaction of PPN synthesis is shown in Figure 5. Pullulan was substituted with phthalic anhydride using hydrophobic interactions and they were dialyzed in order to form self-assembled PPNs.

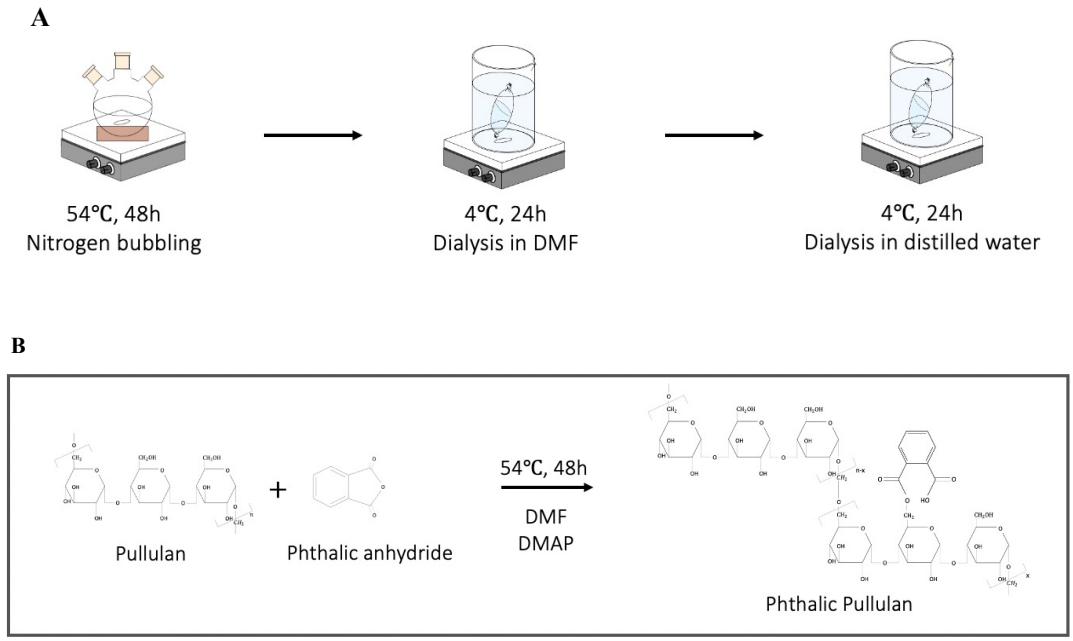

Figure 5. Schematic figure of chemical reaction for the synthesis of PPNs.

The chemical reaction schemes are shown schematically.

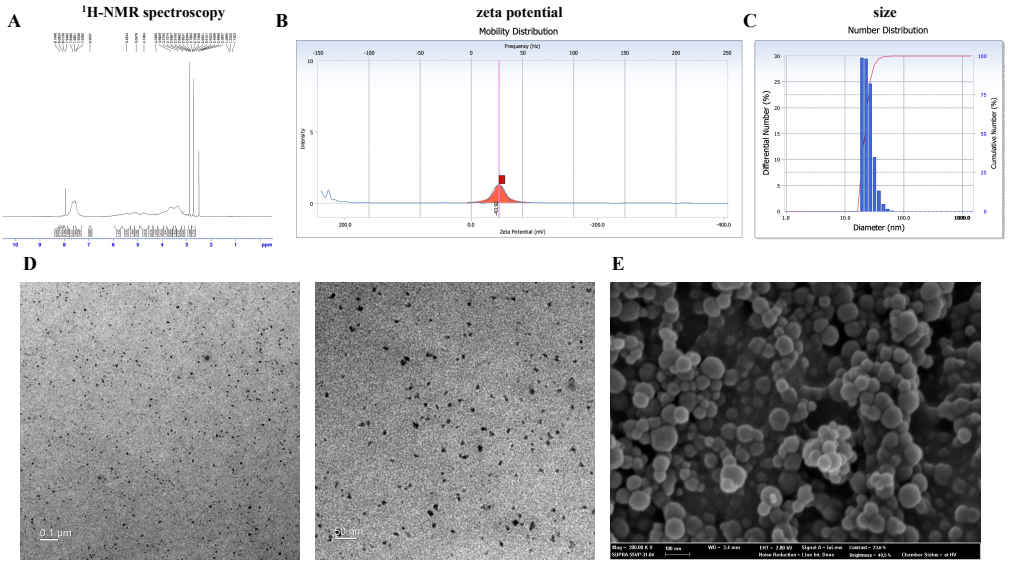

Figure 6. Characteristics of PPNs. PPNs were synthesized from pullulan and phthalic anhydride using hydrophobic interactions and the self-assembly process. (A) Degree of substitution rate of PPN confirmed by ^{1}H-NMR spectroscopy. (B, C) Measurement of zeta potential and size using ELS and DLS, respectively. (D, E) The distribution and morphologies were observed with TEM and SEM.

The substitution rate of phthalic moieties in pullulan was examined by ^{1}H-NMR spectroscopy (Figure 6A) and the degree of substitution rate was calculated as previously mentioned [52]. The ratio of phthalic acid protons (7.4-7.7 ppm) to sugar protons (C1 position of α-1,6 and $a-1,4$ glycosidic bonds-, 4.68 and 5.00 ppm) was calculated as 62.5 mol.%. The zeta potential and size of the PPNs

were examined by using ELS and DLS, respectively. The zeta potential was measured as -41.27 mV (Figure 6B) and the size of the PPN as 70.3 nm (Figure 6C). With TEM, the distribution condition and morphology were checked (Figure 6D). Using SEM, the spherical morphology was confirmed and their size was measured around 100 nm (Figure 6E).

2. Internalization of PPNs into *L. plantarum*

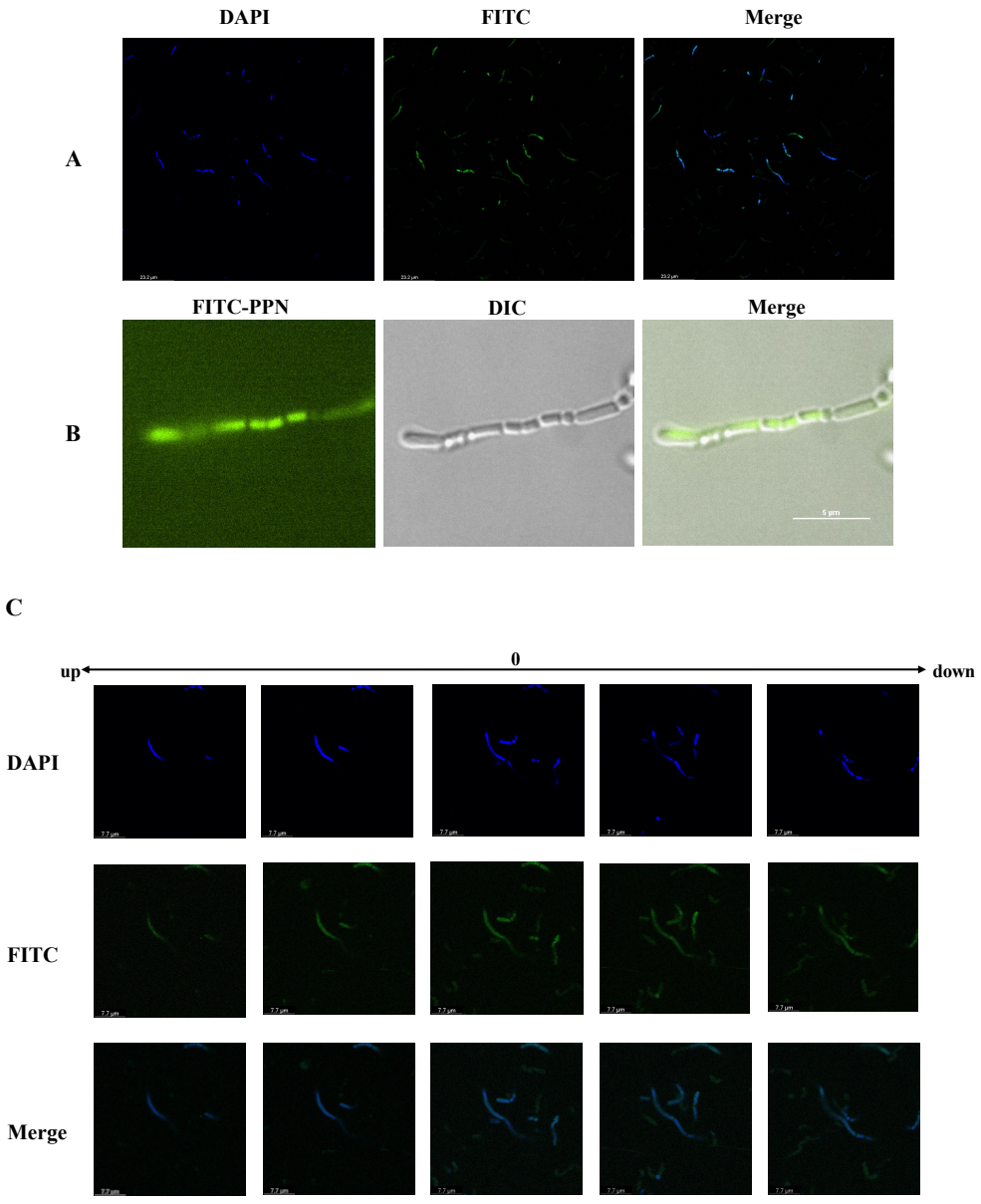

Figure 7. Internalization of PPNs into *L. plantarum*. PPNs were labeled with FITC and their internalization into *L. plantarum* was confirmed. (A)

Internalization was examined by confocal laser scanning microscopy, (B) the fluorescent microscope, and (C) the z-section images showing the internalization of PPNs into *L. plantarum*. Imaging data showing the same results were selected representatively after repeated experiments.

In order to confirm the internalization of PPNs, fluorescence isothiocyanate (FITC) conjugated PPNs were treated to *L. plantarum* for an hour and the internalization was confirmed using the CLSM (Figure 7A). Closer morphology of the PPNs internalized *L. plantarum* was observed by the fluorescent microscope (Figure 7B). Further validation of the internalization, but not the adhesion to the cell wall or the surface, the z-section mode of the CLSM was used and confirmed that intensity of the FITC and DAPI signal was the brightest in the center of the *L. plantarum* (Figure 7C). Collectively, these results confirmed that FITC signals appeared insided the bacteria, suggesting internalization of PPNs into the *L. plantarum*.

3. Synthesis of curcumin-loaded PPNs

The schematic figure of the reaction of the loading of curcumin into the PPNs is shown (Figure 4A).

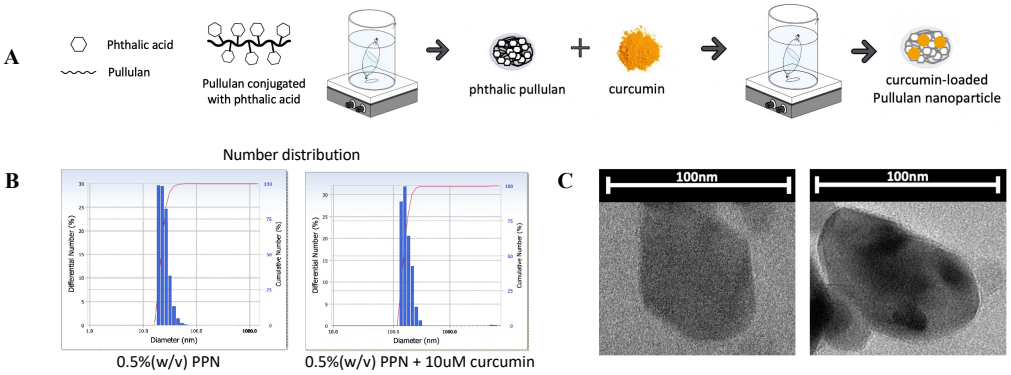

Figure 8. Schematic figure of the synthesis of curcumin-loaded PPNs and their characterization. (A) The schematic figure on the synthesis of curcumin-loaded pullulan nanoparticle using hydrophobic interaction. (B) The size of 10 μM curcumin-loaded PPNs was measured using DLS and (C) the difference in the intensity was observed using TEM. The representative picture from TEM data was selected showing the same results.

The size of 10 μM curcumin-loaded PPNs increased by 174 % compared to PPNs, measured as 192.9 nm (Figure 8B), to which was relative to the increase of concentration of curcumin loaded onto the PPNs, still in the range of the

'nanoparticles' [53]. In order to confirm the loading of curcumin on PPNs, they were observed using TEM. The result shows the difference in intensity where light transmittance differs confirming that curcumin is loaded inside the PPNs (Figure 8C).

4. Curcumin-loaded PPNs induce stress response and plantaricin gene

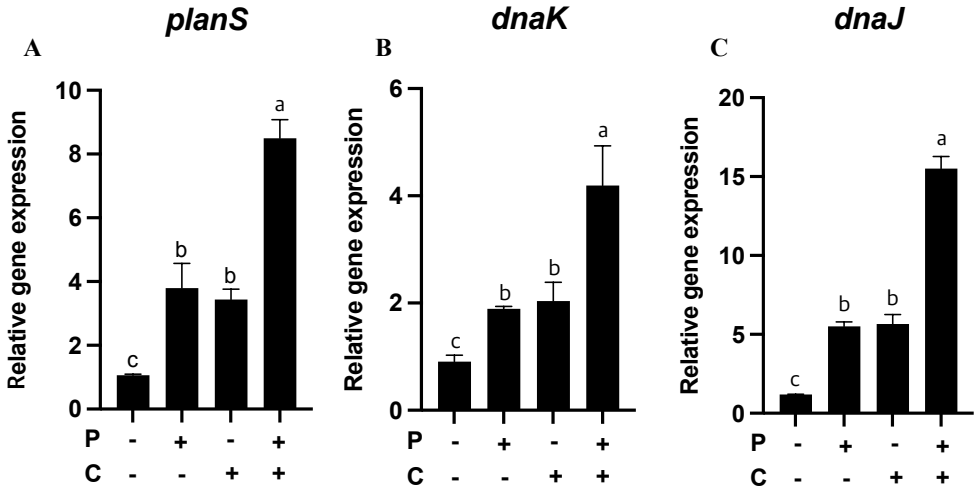

Figure 9. Analysis of genes related to the stress response with *L. plantarum* treated with either PPNs, curcumin, or curcumin-loaded PPNs. *L. plantarum* was treated with each PPNs, curcumin, and curcumin-loaded PPNs and their gene levels of *dnaK, dnaJ*, and *planS* were measured. (A) Releative mRNA expression of *planS* and (B, C) relative expression levels of *dnaK* and *dnaJ* to 16s rRNA was quantified using qRT-PCR. P; nanoparticle [0.5%

PPN(w/v)], C; curcumin 10 μM. Comparisons of the treatments were performed by using one-way analysis of variance (ANOVA) and Tukey's test.

It has been found that PPNs induce a mild stress to *L. plantarum* upregulating stress related genes and consequently, upregulating the *planS* gene expression [32]. Evaluation of plantaricin production in *L. plantarum* was performed by comparing the mRNA expression level to 16S rRNA. *L. plantarum* was each treated with PPNs, curcumin or curcumin-loaded PPNs. The level of *planS* was enhanced the most in the *L. plantarum* treated with curcumin-loaded PPNs (Figure 9A) in accordance with the result of the highest anti-microbial effects in the *L. plantarum* treated with curcumin-loaded PPNs (Figure 9B, 9D). Moreover, the stress regulating gene expression were compared. The expression levels of genes in relation to heat shock proteins, *dnaK* (Figure 9B) and *dnaJ* (Figure 9C) were both higher in curcumin or PPNs treated *L. plantarum* than the control group, and the highest increase was shown in the *L. plantarum* treated with curcumin-loaded PPNs. These results suggested that the curcumin-loaded PPNs internalized in *L. plantarum* upregulated the stress related genes, leading to the production self-defensing bacteriocins, plantaricins.

5. Curcumin-loaded PPNs enhance anti-microbial effects of *L. plantarum*

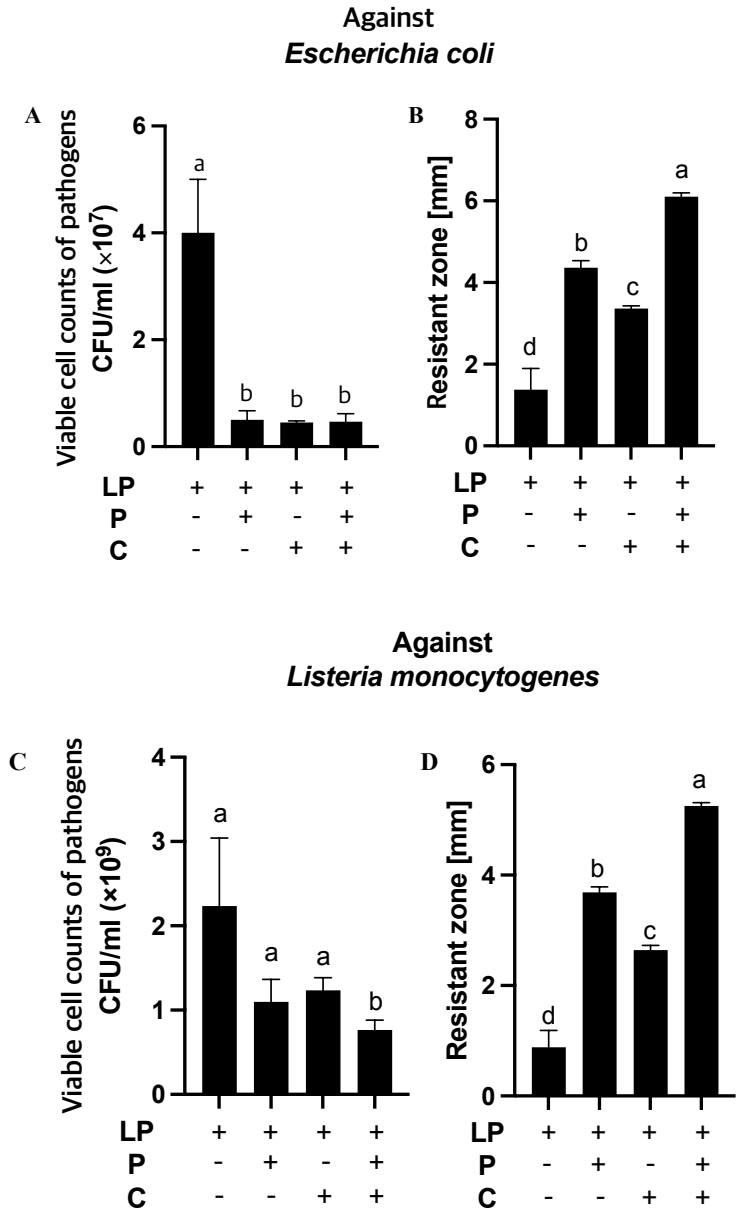

Figure 10. Antimicrobial properties of *L. plantarum* treated either PPNs, curcumin, or curcumin-loaded PPNs. *L. plantarum* treated with either PPNs, curcumin or curcumin-loaded PPNs (shown in Table 4) were cultured with either

(A) *E. coli* or (C) *L. monocytogenes* and the viability was measured by CFU. Likewise, the resistant zone of (B) *E. coli* and (D) *L. monocytogenes* was measured. LP, *L. plantarum*; P, nanoparticle at 0.5% PPN (w/v); C, curcumin at 10 μM). Comparisons of the treatments were performed by using one-way analysis of variance (ANOVA) and Tukey's test.

Table 4. Preparation for the treatment to study anti-microbial effects.

Group	LP	P	C
CON	+	-	-
L. plantarum treated with PPNS	+	+	-
L. plantarum treated with curcumin	+	-	+
L. plantarum treated with curcumin-loaded PPNs	+	+	+

LP, *L. plantarum*; P, nanoparticle at 0.5% PPN (w/v); C, curcumin at 10 μM; CON, control.

In order to test whether the internalization affects the anti-microbial effects, *L. plantarum* was treated with either PPNs, curcumin, or curcumin-loaded PPNs. Enhanced anti-microbial effects were shown in *L. plantarum* treated with curcumin-loaded PPNs in both *E. coli* and *L. monocytogenes* compared to the control group. These anti-microbial properties against these

pathogens were further investigated using the agar diffusion assay (Figure 10A, C). Similarly, resistance zone test showed significantly enhanced resistance activity in curcumin-loaded PPNs internalized *L. plantarum* against *E. coli* and *L. monocytogenes* (Figure 10B, D).

6. Microbial changes in colitis-induced mice treated with LPCP

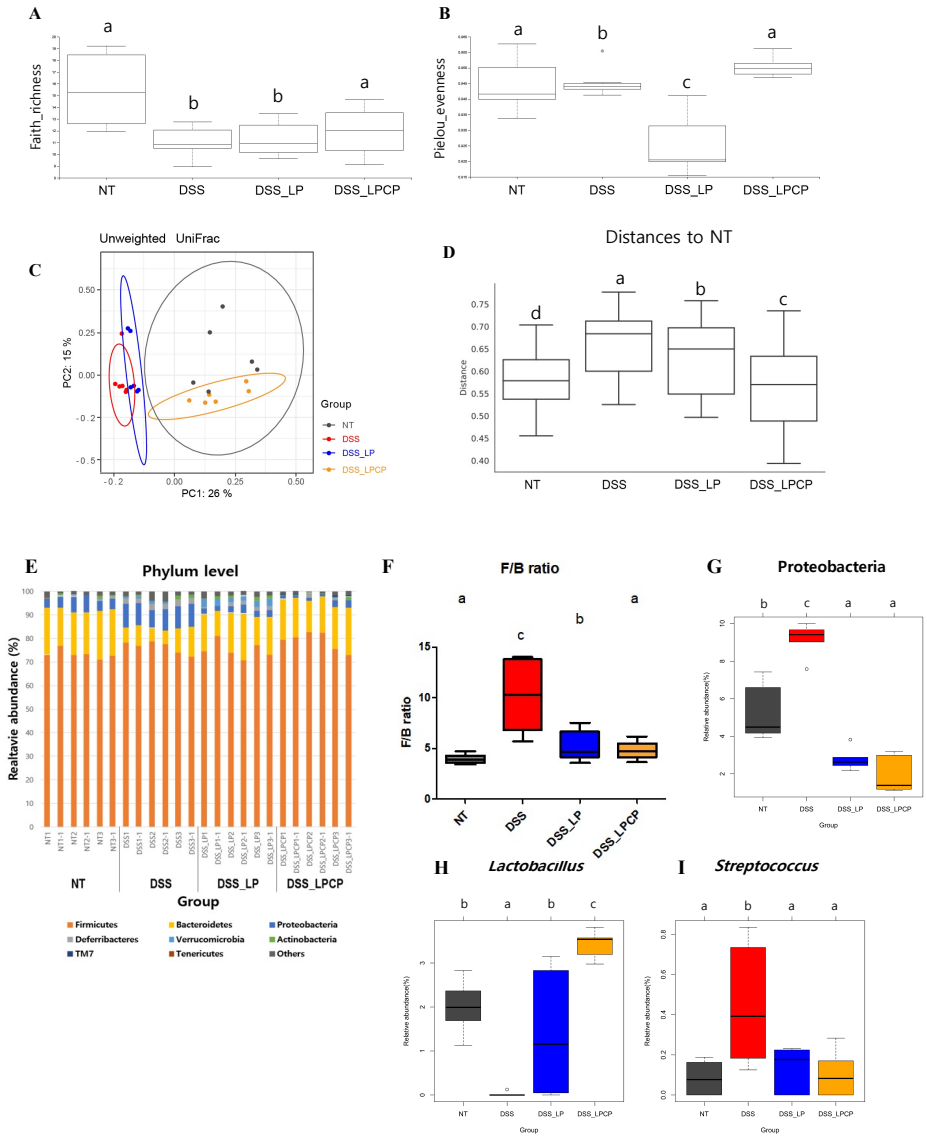

Figure 11. Protective effects of curcumin-loaded PPN internalized *L. plantarum* against colitis-induced microbiome dysruption. Mouse fecal samples were collected and analyzed from each group. (A) α-diversity checked

from richness index and (B) evenness index. (C) Qualitative measure of community dissimilarity was checked with Jaccard distance and (D) their distance to NT was numerically compared and boxplotted. (E) Phylum levels were compared (unclassified phylum was labeled as others), showing (F) F/B ratio and (G) releative abundance of Proteobacteria. Genus levels were also compared and representatively, relative abundance of (H) Lactobacillus and (I) Streptococcus were shown (n=6). Comparisons of the treatments were performed by using one-way analysis of variance (ANOVA) and Tukey's test.

Evaluation of α-diversity was performed using the richness index of Faith's phylogenetic diversity (Figure 11A) and the evenness index of Pielou's evenness (Figure 11B). Richness was highest in the NT group, and DSS-treated groups showed a relatively low richness while the LPCP group showed relatively higher tendency. Also, in the case of evenness, group treated with DSS and LP showed the least, and the group treated with DSS and LPCP showed the highest eveness among the groups. Compared to the NT group, DSS treatment lowered the richness and evenness was recovered in the group trated with LPCP. To confirm the samples' qualtitative measure of community dissimilarity that incorporates phylogenetic relationships between the features, β-diversity was evaluated. NT group and the group treated with DSS and LPCP clustered together, while the

DSS, DSS with LP group clustered together (Figure 11C). The LPCP group showed the most similar microbiome constitution witht the NT group. The β-diversity was also numerically boxplotted (Figure 11D) and compared and likewise the results of the PCoA, NT group's distance was furthest with the DSS treatment group, while they were most closest to the LPCP group. It was confirmed that LPCP group showed closest microbiome composition to the NT group with the results above. Taxonomy assignmnet was performed and phylum (Figure 11E), genus level was compared. The F/B(Firmicutes/Bacteriodetes) ratio from was shown the highest in the DSS treated group and no significance was found in the NT, DSS with LP and the DSS with LPCP groups (Figure 11F). Proteobacteria level is closesly related to the susceptibilty [54, 55] to colitis so their levels were checked and showed that they showed the lowest relative abundance compared to the NT group (figure 11G). 41 genera showed significant difference between the groups, and representatively, the *Lactobacillus* (Figure 11H) and the *Streptococcus* (Figure 11I) group was shown. The Lactobacillus showed the highest relative abundance in the DSS treated LPCP group, while showing the least relative abundance of the *Streptococcus* genus.

7. Physiological changes in colitis-induced mice treated with LPCP

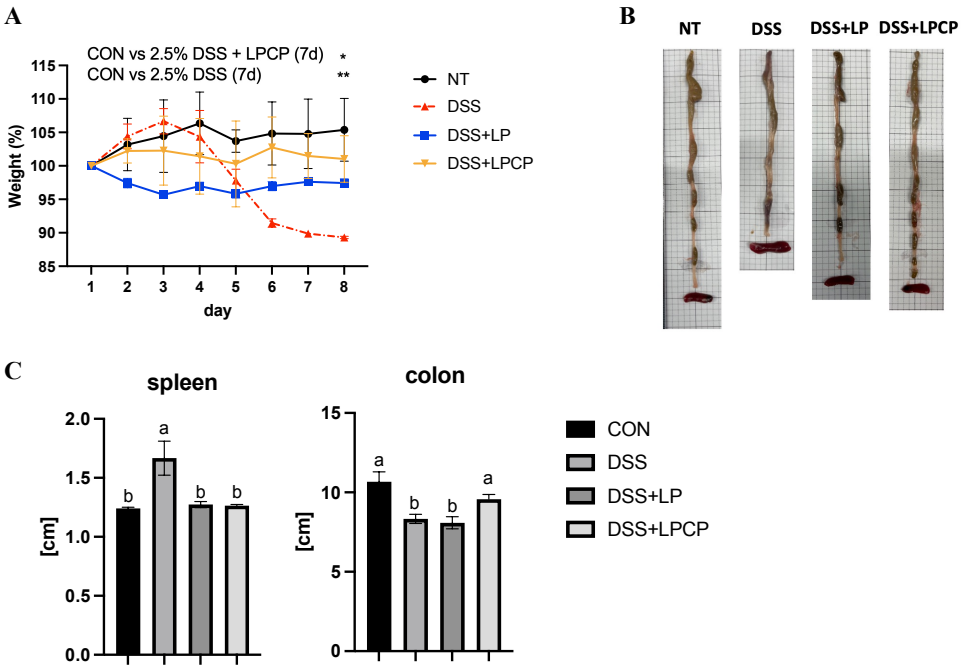

Figure 12. Changes on body weight and the length of colon and spleen in mice treated with LPCP. Mice were induced colitis with DSS and treated with *L. plantarum* and LPCP. Their weight loss and length of spleen and colone were measured. (A) Weight loss (%) was measured for 7 days after DSS treatment. (B, C) Mice from each group was sacrificed and their colon and spleen length were measured (n=6). Comparisons of the treatments were performed by using one-way analysis of variance (ANOVA) and Tukey's test.

Table 5. Treatment for the group of colitis-induced mice.

Group	treatment
NT	No treatment
DSS	2.5% DSS treated for 7 days
DSS+LP	*L. plantarum* pretreatment for 7 days + *L. plantarum* and DSS treatment for 7 days (total 14 days)
DSS+LPCP	LPCP pretreatment for 7 days + LPCP and DSS treatment for 7 days (total 14 days)

Mice were pretreated with *L. plantarum* or LPCP for 7 days before DSS treatment and after the treatment for 7 days. It has been suggested that pretreatment of probiotics for 7 days could maintain epithelial integrity and also attenuates pro-inflammatory cytokine levels. After DSS treatment for 7 days, their weight loss were measured (Figure 12A). Length of their colon and spleen was reduced in DSS treated group (Figure 12B, C). In case of the group treated with DSS and LPCP, their length was and showed a no significant change when compared with the NT group.

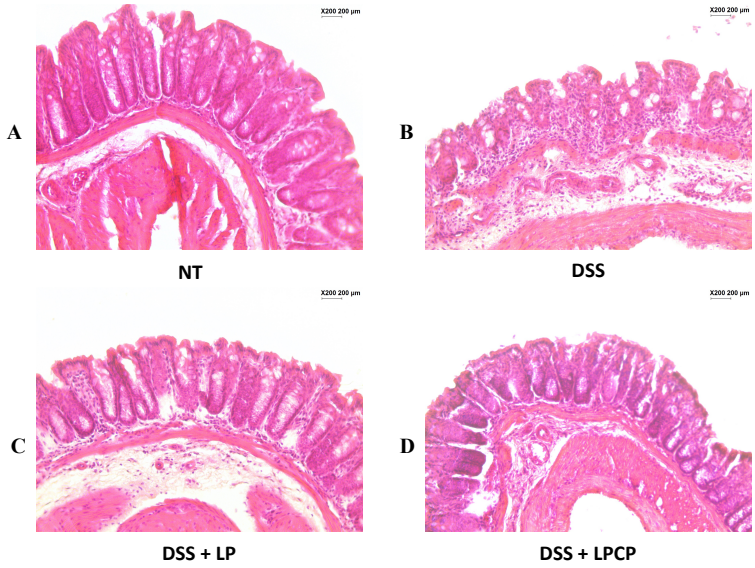

Figure 13. Histology of the large intestine from colitis-induced mice treated with LPCP. Mice with DSS-induced colitis were treated with LP or LPCP. The large intestine taken from mouse was perfused and fixed with 4 % paraformaldehyde and embedded into paraffin block for hematoxylin and eosin (H&E) staining. The representative histological picture showing the large intestine from (A) NT, (B) DSS, (C) DSS+LP, (D) DSS+LPCP.

Moreover, the histological data from large intestine showed that the damage was the most severe in the DSS treated group (Figure 13B). Both groups, DSS+LP (Figure 13C) and DSS+LPCP (Figure 13D) showed similar morphologies compared to the NT group (Figure 13A).

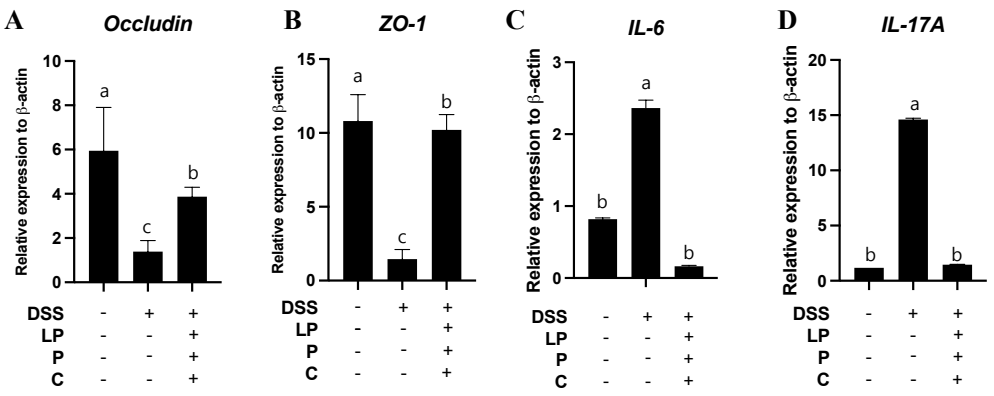

Figure 14. Changes of tight junction proteins and pro-inflammatory cytokines in intestine homogenate from colitis induced mice treated with LPCP. Mice with DSS-induced colitis were treated with LP or LPCP. The intestine from each mouse was homogenized in trizol overnight. Intestine tissue homogenates were collected and mRNA were extraced for qRT-PCR analysis. Expression of Occludin, ZO-1, IL-6, and IL-17A were compared. (A, B) Tight junction regulating genes (occludin and ZO-1) and (C, D) inflammatory cytokines (IL-6 and IL17A) were examined at gene level expression using qRT-PCR. Comparisons of the treatments were performed by using one-way analysis of variance (ANOVA) and Tukey's test.

Occludin and ZO-1 genes that regulate the tight junction proteins were examined using the qRT-PCR (Figure 14A, B). In the DSS+LPCP group, tight junction gene expressions were enhanced. Likewise, inflammatory cytokines, IL-

6 and IL-17A showed significantly low levels in DSS+LPCP groups (Figure 14C, D) suggesting a potential of LPCP treatment enhancing the barrier functions.

V. Discussion

Inflammatory Bowel Disease (IBD), a group of chronic inflammatory disease of the gastrointestinal tract, is the confluence of genetic, microbial and environmental factors that alter gut homeostasis [23], thereby triggering immune mediated inflammation. IBD can be developed when pathobiont accumulation occurs [56]. Patients with IBD loses beneficial symbionts, and then pathobiont expansion occurs leading to decreased microbial diversity [57]. Therefore, among the promising treatments against IBD, the 'probiotics' treatment in order to balance the microbial diversity of the host, has been studied and carried out actively [47, 58]. In this study, curcumin-loaded PPNs were used as 'prebiotics' to enhance the antimicrobial activities of *L. plantarum*.

Prebiotics are defined as compounds that are non-digestible and stimulates the activity of probiotics and other live organisms in the GI tract that confers beneficial effects on the host [59]. In this study, curcumin-loaded PPNs were suggested as a new formula to prebiotics. Polymeric nanoparticles' internalization into mammalian cells through the endocytosis process has been previously elucidated [21, 60], however, their internalization into prokaryotes as prebiotics is still in their early stage. Although internalization of PPNs has been observed [32], a precise mechanism has not been elucidated in detail. Polymeric

nanoparticles also hold benefits in that they can load hydrophobic drugs overcoming biological barriers [61]. Therefore, this study has advantage in a new aspect of curcumin-loaded PPNs used as prebiotics to L. *plantarum*. At this end, curcumin-loaded PPNs were synthesized and internalized into *L. plantarum* expecting enhanced microbial activities of *L. plantarum.*

The aim of the present study was to elucidate the enhanced protective effect of *L. plantarum* that had been internalized with curcumin-loaded PPNs against microbial disruption and their contribution to alleviating colitis. Microbial diversity was enhanced with oral treatment of *L. plantarum* internalized with curcumin-loaded PPNs and the pro-inflammatory cytokines in the intestine were suppressed. IL-17A production was inhibited by treatment with *L. plantarum* internalized with curcumin-loaded PPNs in the present study supporting the idea that suppression of IL-17A may ameliorate colitis symptoms [62]. These results suggest a therapeutic potential of *L. plantarum* internalized with curcumin-loaded PPNs to treat IBD. Indeed, there was a study claiming that alleviation of colitis may be a result of *Lactobacillus* contributing to the increase of regulatory T cells in colonic tissues [63], but this idea needs to be further investigated in this study.

The present study carries a shortcoming as the exact internalization mechanism and how curcumin-loaded on PPNs is released, and their direct effect

on the host are yet to be known. Moreover, *L. plantarum* internalized with curcumin-loaded PPNs are not working solely to contribute to the microbial diversity and alleviation of colitis. For instance, microbiome composition is recently suggested to affect the regulation of regulatory T cells [64] and functions of lymphoid cells [65]. The interactions of immune cell networks need to be also further clarified.

To summarize, *L. plantarum* internalized with curcumin-loaded PPNs inhibited the viability of particular pathogens contributing to the maintenance of the diversity of microbiota in the intestinal flora. They enhanced the intestinal tract's stability suppressing production of pro-inflammatory cytokines suggesting curcumin-internalized L. plantarum as a possible therapeutic agent.

VI. Literature Cited

1. Lee, W.H., et al., *Curcumin and its derivatives: their application in neuropharmacology and neuroscience in the 21st century.* Curr Neuropharmacol, 2013. **11**(4): p. 338-78.
2. Aggarwal, B.B. and K.B. Harikumar, *Potential therapeutic effects of curcumin, the anti-inflammatory agent, against neurodegenerative, cardiovascular, pulmonary, metabolic, autoimmune and neoplastic diseases.* Int J Biochem Cell Biol, 2009. **41**(1): p. 40-59.
3. Singh, S. and B.B. Aggarwal, *Activation of transcription factor NF-kappa B is suppressed by curcumin (diferuloylmethane) [corrected].* J Biol Chem, 1995. **270**(42): p. 24995-5000.
4. Kotha, R.R. and D.L. Luthria, *Curcumin: Biological, Pharmaceutical, Nutraceutical, and Analytical Aspects.* Molecules, 2019. **24**(16).
5. Shanmugam, M.K., et al., *The multifaceted role of curcumin in cancer prevention and treatment.* Molecules, 2015. **20**(2): p. 2728-69.
6. Chuengsamarn, S., et al., *Curcumin extract for prevention of type 2 diabetes.* Diabetes Care, 2012. **35**(11): p. 2121-7.
7. Zhu, T., et al., *Curcumin Attenuates Asthmatic Airway Inflammation and Mucus Hypersecretion Involving a PPARgamma-Dependent NF-kappaB Signaling Pathway In Vivo and In Vitro.* Mediators Inflamm, 2019. **2019**: p. 4927430.
8. Yin, H., et al., *Curcumin Suppresses IL-1beta Secretion and Prevents Inflammation through Inhibition of the NLRP3 Inflammasome.* J Immunol, 2018. **200**(8): p. 2835-2846.

9. Yin, H.P., et al., *Curcumin Suppresses IL-1 beta Secretion and Prevents Inflammation through Inhibition of the NLRP3 Inflammasome.* Journal of Immunology, 2018. **200**(8): p. 2835-2846.
10. Zhao, H.M., et al., *Curcumin Suppressed Activation of Dendritic Cells via JAK/STAT/SOCS Signal in Mice with Experimental Colitis.* Front Pharmacol, 2016. **7**: p. 455.
11. Hamaguchi, T., K. Ono, and M. Yamada, *REVIEW: Curcumin and Alzheimer's disease.* CNS Neurosci Ther, 2010. **16**(5): p. 285-97.
12. Bawa, R., et al., *Self-assembling peptide-based nanoparticles enhance cellular delivery of the hydrophobic anticancer drug ellipticine through caveolae-dependent endocytosis.* Nanomedicine, 2012. **8**(5): p. 647-54.
13. Yavarpour-Bali, H., M. Ghasemi-Kasman, and M. Pirzadeh, *Curcumin-loaded nanoparticles: a novel therapeutic strategy in treatment of central nervous system disorders.* Int J Nanomedicine, 2019. **14**: p. 4449-4460.
14. Sun, T., et al., *Engineered nanoparticles for drug delivery in cancer therapy.* Angew Chem Int Ed Engl, 2014. **53**(46): p. 12320-64.
15. Liu, W., et al., *Oral bioavailability of curcumin: problems and advancements.* J Drug Target, 2016. **24**(8): p. 694-702.
16. Mitchell, M.J., et al., *Engineering precision nanoparticles for drug delivery.* Nat Rev Drug Discov, 2021. **20**(2): p. 101-124.
17. Rhee, M., et al., *Synthesis of size-tunable polymeric nanoparticles enabled by 3D hydrodynamic flow focusing in single-layer microchannels.* Adv Mater, 2011. **23**(12): p. H79-83.
18. Wei, C.H.N. and Q.M. Liu, *Shape-, size-, and density-tunable synthesis and optical properties of copper nanoparticles.* Crystengcomm, 2017. **19**(24): p. 3254-3262.

19. Ferri, F., et al., *Nanoparticle size distribution from inversion of wide angle X-ray total scattering data.* Sci Rep, 2020. **10**(1): p. 12759.
20. Mout, R., et al., *Surface functionalization of nanoparticles for nanomedicine.* Chem Soc Rev, 2012. **41**(7): p. 2539-44.
21. Oh, N. and J.H. Park, *Endocytosis and exocytosis of nanoparticles in mammalian cells.* Int J Nanomedicine, 2014. **9 Suppl 1**: p. 51-63.
22. Patra, J.K., et al., *Nano based drug delivery systems: recent developments and future prospects.* J Nanobiotechnology, 2018. **16**(1): p. 71.
23. Rangan, P., et al., *Fasting-Mimicking Diet Modulates Microbiota and Promotes Intestinal Regeneration to Reduce Inflammatory Bowel Disease Pathology.* Cell Rep, 2019. **26**(10): p. 2704-2719 e6.
24. Altajar, S. and A. Moss, *Inflammatory Bowel Disease Environmental Risk Factors: Diet and Gut Microbiota.* Curr Gastroenterol Rep, 2020. **22**(12): p. 57.
25. Chassaing, B., et al., *Dextran sulfate sodium (DSS)-induced colitis in mice.* Curr Protoc Immunol, 2014. **104**: p. 15 25 1-15 25 14.
26. Coleman, O.I. and D. Haller, *Bacterial Signaling at the Intestinal Epithelial Interface in Inflammation and Cancer.* Front Immunol, 2017. **8**: p. 1927.
27. Bested, A.C., A.C. Logan, and E.M. Selhub, *Intestinal microbiota, probiotics and mental health: from Metchnikoff to modern advances: Part I - autointoxication revisited.* Gut Pathog, 2013. **5**(1): p. 5.
28. Stofilova, J., et al., *Cytokine production in vitro and in rat model of colitis in response to Lactobacillus plantarum LS/07.* Biomed Pharmacother, 2017. **94**: p. 1176-1185.
29. Le, B. and S.H. Yang, *Efficacy of Lactobacillus plantarum in prevention of inflammatory bowel disease.* Toxicol Rep, 2018. **5**: p. 314-317.

30. Markowiak, P. and K. Slizewska, *Effects of Probiotics, Prebiotics, and Synbiotics on Human Health.* Nutrients, 2017. **9**(9).
31. Cheng, K.C., A. Demirci, and J.M. Catchmark, *Pullulan: biosynthesis, production, and applications.* Appl Microbiol Biotechnol, 2011. **92**(1): p. 29-44.
32. Hong, L., et al., *Pullulan Nanoparticles as Prebiotics Enhance the Antibacterial Properties of Lactobacillus plantarum Through the Induction of Mild Stress in Probiotics.* Front Microbiol, 2019. **10**: p. 142.
33. Gutierrez-Cortes, C., et al., *Enhanced Bacteriocin Production by Pediococcus pentosaceus 147 in Co-culture With Lactobacillus plantarum LE27 on Cheese Whey Broth.* Front Microbiol, 2018. **9**: p. 2952.
34. Kumariya, R., et al., *Bacteriocins: Classification, synthesis, mechanism of action and resistance development in food spoilage causing bacteria.* Microb Pathog, 2019. **128**: p. 171-177.
35. M'Koma, A.E., *Inflammatory bowel disease: an expanding global health problem.* Clin Med Insights Gastroenterol, 2013. **6**: p. 33-47.
36. Kaplan, G.G. and S.C. Ng, *Understanding and Preventing the Global Increase of Inflammatory Bowel Disease.* Gastroenterology, 2017. **152**(2): p. 313-321 e2.
37. Rubin, D.T. and S.B. Hanauer, *Smoking and inflammatory bowel disease.* Eur J Gastroenterol Hepatol, 2000. **12**(8): p. 855-62.
38. Rubin, D.C., A. Shaker, and M.S. Levin, *Chronic intestinal inflammation: inflammatory bowel disease and colitis-associated colon cancer.* Front Immunol, 2012. **3**: p. 107.
39. Nitzan, O., et al., *Role of antibiotics for treatment of inflammatory bowel disease.* World J Gastroenterol, 2016. **22**(3): p. 1078-87.

40. Sica, G.S. and L. Biancone, *Surgery for inflammatory bowel disease in the era of laparoscopy.* World J Gastroenterol, 2013. **19**(16): p. 2445-8.
41. Caruso, R., B.C. Lo, and G. Nunez, *Host-microbiota interactions in inflammatory bowel disease.* Nat Rev Immunol, 2020. **20**(7): p. 411-426.
42. Oh, N.S., et al., *Probiotic and anti-inflammatory potential of Lactobacillus rhamnosus 4B15 and Lactobacillus gasseri 4M13 isolated from infant feces.* PLoS One, 2018. **13**(2): p. e0192021.
43. Mennigen, R., et al., *Probiotic mixture VSL#3 protects the epithelial barrier by maintaining tight junction protein expression and preventing apoptosis in a murine model of colitis.* Am J Physiol Gastrointest Liver Physiol, 2009. **296**(5): p. G1140-9.
44. Guandalini, S. and N. Sansotta, *Probiotics in the Treatment of Inflammatory Bowel Disease.* Adv Exp Med Biol, 2019. **1125**: p. 101-107.
45. Orel, R. and T. Kamhi Trop, *Intestinal microbiota, probiotics and prebiotics in inflammatory bowel disease.* World J Gastroenterol, 2014. **20**(33): p. 11505-24.
46. Scaldaferri, F., et al., *Gut microbial flora, prebiotics, and probiotics in IBD: their current usage and utility.* Biomed Res Int, 2013. **2013**: p. 435268.
47. Zhang, F., et al., *The Impact of Lactobacillus plantarum on the Gut Microbiota of Mice with DSS-Induced Colitis.* Biomed Res Int, 2019. **2019**: p. 3921315.
48. Son, S.J., et al., *Effect of the Lactobacillus rhamnosus strain GG and tagatose as a synbiotic combination in a dextran sulfate sodium-induced colitis murine model.* J Dairy Sci, 2019. **102**(4): p. 2844-2853.

49. Simeoli, R., et al., *Preventive and therapeutic effects of Lactobacillus paracasei B21060-based synbiotic treatment on gut inflammation and barrier integrity in colitic mice.* J Nutr, 2015. **145**(6): p. 1202-10.
50. Ditu, L.M., et al., *Modulation of virulence and antibiotic susceptibility of enteropathogenic Escherichia coli strains by Enterococcus faecium probiotic strain culture fractions.* Anaerobe, 2011. **17**(6): p. 448-51.
51. O'Driscoll, N.H., et al., *Production and evaluation of an antimicrobial peptide-containing wafer formulation for topical application.* Curr Microbiol, 2013. **66**(3): p. 271-8.
52. Tao, X., et al., *Cholesterol-Modified Amino-Pullulan Nanoparticles as a Drug Carrier: Comparative Study of Cholesterol-Modified Carboxyethyl Pullulan and Pullulan Nanoparticles.* Nanomaterials (Basel), 2016. **6**(9).
53. Prabha, S., et al., *Effect of size on biological properties of nanoparticles employed in gene delivery.* Artif Cells Nanomed Biotechnol, 2016. **44**(1): p. 83-91.
54. Roy, U., et al., *Distinct Microbial Communities Trigger Colitis Development upon Intestinal Barrier Damage via Innate or Adaptive Immune Cells.* Cell Reports, 2017. **21**(4): p. 994-1008.
55. Shin, N.R., T.W. Whon, and J.W. Bae, *Proteobacteria: microbial signature of dysbiosis in gut microbiota.* Trends in Biotechnology, 2015. **33**(9): p. 496-503.
56. Anbazhagan, A.N., et al., *Pathophysiology of IBD associated diarrhea.* Tissue Barriers, 2018. **6**(2): p. e1463897.
57. Gong, D., et al., *Involvement of Reduced Microbial Diversity in Inflammatory Bowel Disease.* Gastroenterol Res Pract, 2016. **2016**: p. 6951091.

58. Kim, W.K., et al., *Alleviation of DSS-induced colitis via Lactobacillus acidophilus treatment in mice.* Food Funct, 2021. **12**(1): p. 340-350.
59. Gibson, G.R., *Dietary modulation of the human gut microflora using the prebiotics oligofructose and inulin.* J Nutr, 1999. **129**(7 Suppl): p. 1438S-41S.
60. Nelemans, L.C. and L. Gurevich, *Drug Delivery with Polymeric Nanocarriers-Cellular Uptake Mechanisms.* Materials (Basel), 2020. **13**(2).
61. Blanco, E., H. Shen, and M. Ferrari, *Principles of nanoparticle design for overcoming biological barriers to drug delivery.* Nat Biotechnol, 2015. **33**(9): p. 941-51.
62. Hyun, Y.S., et al., *Role of IL-17A in the development of colitis-associated cancer.* Carcinogenesis, 2012. **33**(4): p. 931-6.
63. Kwon, H.K., et al., *Generation of regulatory dendritic cells and CD4+Foxp3+ T cells by probiotics administration suppresses immune disorders.* Proc Natl Acad Sci U S A, 2010. **107**(5): p. 2159-64.
64. Pandiyan, P., et al., *Microbiome Dependent Regulation of Tregs and Th17 Cells in Mucosa.* Front Immunol, 2019. **10**: p. 426.
65. Kamada, N. and G. Nunez, *Role of the gut microbiota in the development and function of lymphoid cells.* J Immunol, 2013. **190**(4): p. 1389-95.

VII. Summary in Korean

프로바이오틱스 (probiotics)는 적정량 투여 시, 숙주에게 건강상의 이점을 주는 살아 있는 미생물을 의미한다.프리바이오틱스 (prebiotics)는 일반적으로 숙주에게는 소화/흡수되지 않으며 위장관에서 유익균의 성장 또는 활동을 자극할 수 있는 물질로 정의되는데, 본 연구에서는 프탈릴 플루란 나노입자 (phthalyl pullulan nanoparticle)를 합성하여 프리바이오틱스 실험을 진행하였다.

면역 조절 물질로 알려진 커큐민 (curcumin)을 플루란 나노입자에 소수성 상호작용을 통해 담지하여, 유산균인 락토바실러스 플란타룸 (*Lactobacillus plantarum*)에 도입하였다. 이는스트레스 조절 유전자인 dnaK 와 dnaJ 의 발현을 유도와 함께락토바실러스 플란타룸 균에서 만들어지는 항균 물질인 플란타리신의 증가를 *planS* 유전자 발현을 통해 검증하였다. 본 연구에서 그람 음성균인 대장균과 그람 양성균인 리스테리아균에 대한 항균 효과를 확인하였다.

장내 균총 조성 변화 및 면역학적 효과를 확인하기 위해 DSS 로 마우스에 장염을 유도하여 장벽 손상 및 균총 변화를 확인하고 프리바이오틱스가 도입된 유산균주를 처리하여 예방 효과를 확인하였다. 도입이 안된것은 어떻다는 것을 함께 설명 + 프리바이오틱스가 도입된 유산균이 처리된 마우스 그룹이 음성 대조군과 가장 비슷한 균총 조성을 가지는 것을 균총 분석을 통해 확인하였다.

장염이 현상적으로 예방되는 것을 몸무게 변화, 콜론과 비장의 길이 변화를 음성 대조군과의 비교를 통해 확인하였으며, 나아가 장벽 손상 또한 예방 되는 것을 확인하였다.

세포 결합 관련 단백질들인 Occludin, ZO-과 장 조직에서의 IL-6, IL-17A 등 염증성 사이토카인의 발현이 감소하는 것을 mRNA 수준에서 확인하였다.

해당 연구에서는 커큐민이 담지된 플루란 나노입자를 락토바실러스 플란타룸 균에 주입시켜 발생하는 플란타리신에 의한 항균효과를 확인하였다. 마우스 개체 체내에서 유산 균총 다양성 유지에 기여하는 것을 검증하였으며, 장염 유도 마우스에서 현상적으로 장염이 완화되는 것을 확인한 연구이다.